REMOTE SENS. ENVIRON. 49:246–263 (1994)

Estimating Crop Water Deficit Using the Relation between Surface–Air Temperature and Spectral Vegetation Index

M. S. Moran, T. R. Clarke,* Y. Inoue,† and A. Vidal‡*

The crop water stress index (CWSI), developed at the USDA-ARS U.S. Water Conservation Laboratory, Phoenix, Arizona, is a commonly used index for detection of plant stress based on the difference between foliage and air temperature. Application of CWSI at local and regional scales has been hampered by the difficulty of measuring foliage temperature of partially vegetated fields. Most hand-held, airborne, and satellite-based infrared sensors measure a composite of both the soil and plant temperatures. The concept proposed here, termed the vegetation index/temperature (VIT) trapezoid, is an attempt to combine spectral vegetation indices with composite surface temperature measurements to allow application of the CWSI theory to partially-vegetated fields without knowledge of foliage temperature. Based on this approach, a new index [water deficit index (WDI)] was introduced for evaluating evapotranspiration rates of both full-cover and partially vegetated sites. By definition, WDI is related to the ratio of actual and potential evapotranspiration; in practice, WDI can be computed using remotely sensed measurements of surface temperature and reflectance (red and near-infrared spectrum) with limited on-site meteorological data (net radiation, vapor pressure deficit, wind speed, and air temperature). Both the VIT trapezoid and WDI concepts were evaluated using 1) a simulation of a two-component (soil and vegetation) energy balance model and 2) existing data from an experiment in an alfalfa field in Phoenix, Arizona. Results from both studies showed that the WDI provided accurate estimates of field evapotranspiration rates and relative field water deficit for both full-cover and partially vegetated sites.

INTRODUCTION

There are numerous experimental and theoretical studies addressing the use of plant foliage temperature to gain information about a variety of plant and soil properties (e.g., Tanner, 1963; Jackson, 1982; Idso et al., 1986). In these studies, foliage temperature has been related to soil moisture content (Jackson et al., 1977a; Jackson, 1982), plant water stress (Jackson et al., 1977b; Idso et al., 1978; Jackson and Pinter, 1981), and plant transpiration rate (Idso et al., 1977a; Jackson et al., 1983). An important contribution of this research was the creation of the Idso–Jackson crop water stress index (CWSI) (Idso et al., 1981; Jackson et al., 1981). Based primarily on plant foliage temperatures, this index has been shown to be closely correlated with soil moisture content, soil water matrix potential, soil salinity, soil waterlogging, plant water potential, leaf diffusion resistance, and photosynthesis, as well as final crop yield [see historical reviews by Jackson (1987) and Idso et al. (1986)]. These research results led to the use of CWSI for such important farm applications as irrigation scheduling, predicting crop yields, and detecting certain plant diseases (Jackson et al., 1977b; 1980; Idso et al., 1977b; Reginato et al., 1978; Pinter et al., 1979).

Despite its ubiquitous nature, application of the CWSI at local and regional scales has been hampered by the difficulty of measuring foliage temperature in partially vegetated fields. Hand-held infrared thermome-

*USDA-ARS U.S. Water Conservation Laboratory, Phoenix
†NIAES, Division of Information Analysis, Laboratory of Agro-Biological Measurements, Tsukuba, Japan
‡CEMAGREF-ENGREF Remote Sensing Laboratory, Montpellier, France

Address correspondence to Susan Moran, USDA-ARS-SWRC, 2000 E. Allen Rd., Tucson, AZ 85719.
Received 7 May 1993; revised 20 April 1994.

0034-4257/94/$7.00

ters (IRT) and most airborne and satellite-based infrared sensors measure a composite of both the soil and plant temperatures. When vegetation is sparse, the temperature of the soil dominates the composite temperature measurement and negates any possibility of applying the CWSI using IRT measurements. In fact, Jackson et al. (1981) warned that

> "it is important that the soil background *not* appear in the field of view of the infrared thermometer. Soil temperatures can be drastically different from plant temperatures, and their inclusion can cause serious errors in the CWSI."

The approach proposed here, termed the vegetation index / temperature (VIT) trapezoid, is an attempt to combine spectral vegetation indices with composite surface temperature measurements to allow application of the CWSI theory to partially vegetated fields without *a priori* knowledge of the percent vegetation cover. The approach capitalizes on two considerations: 1) Values of many properties are easier to compute for the extremes (full-cover and bare soil) than for intermediate points, and 2) many of the basic theoretical concepts of the CWSI have a near-linear relation with percent vegetation cover. Consequently, linear interpolations between properties computed for full-cover and bare soil condi-

Table 1. Summary of Scientific and Technical Notation

C_v	= volumetric heat capacity of air (J °C^{-1} m^{-3})
Δ	= slope of the saturated vapor pressure-temperature relation (kPa °C^{-1})
d_o	= displacement height (m)
e_a	= vapor pressure of the air (kPa)
e^*	= saturated vapor pressure at $(T_c + T_a)/2$ (kPa)
e_b^*	= saturated vapor pressure at $(T_a + f_0)$ (kPa)
E_Γ	= evapotranspiration rate (mm h^{-1})
E_{Γ_p}	= potential evapotranspiration rate (mm h^{-1})
E	= evaporation rate (mm h^{-1})
f_1, f_0	= slope (°C kPa^{-1}) and offset (°C) of relation between $(T_c - T_a)$ and VPD for a well-watered crop
γ	= psychrometric constant (kPa °C^{-1})
γ^*	= $\gamma(1 + r_{cp}/r_a)$ (kPa °C^{-1})
Γ	= transpiration rate (mm h^{-1})
G	= soil heat flux density (W m^{-2})
h	= plant height or roughness element height (m)
H	= sensible heat flux density (W m^{-2})
k	= von Karman's constant (≈ 0.4)
kB^{-1}	= $\ln(z_{om}/z_{oh})$ (unitless)
λE_γ	= latent heat flux density (W m^{-2})
λ	= heat of vaporization (J kg^{-1})
LAI	= leaf area index (m^{2}m^{-2})
Ψ_h	= stability correction for heat (unitless)
Ψ_m	= stability correction for momentum (unitless)
r_a	= aerodynamic resistance (s m^{-1})
r_c	= canopy resistance to vapor transport (s m^{-1})
r_{cx}	= maximum canopy resistance, associated with nearly complete stomatal closure (s m^{-1})
r_{cp}	= canopy resistance at potential evapotranspiration (s m^{-1})
r_{cm}	= minimum canopy resistance, where $r_{cm} = r_{cp}$ (s m^{-1})
r_s	= stomatal resistance (s m^{-1})
r_{sx}	= maximum stomatal resistance (s m^{-1})
r_{sp}	= stomatal resistance at potential evapotranspiration (s m^{-1})
r_{sm}	= minimum stomatal resistance, where $r_{sm} = r_{sp}$ (s m^{-1})
r_{co}	= resistance to sensible heat transfer for full-cover vegetation per surface unit (s m^{-1})
r_{oo}	= resistance to sensible heat transfer for bare soil per surface unit (s m^{-1})
R_n	= net radiant heat flux density (W m^{-2})
T_a	= air temperature (°C)
T_c	= crop foliage temperature (°C)
T_o	= soil surface temperature (°C)
T_s	= surface composite temperature (a weighted average of T_o and T_c) (°C)
U	= wind speed (m s^{-1})
V_c	= vegetation cover (ranging from 0 = no vegetation to 1 = full vegetation cover)
VPD	= $(e^* - e_a)$, vapor pressure deficit of the air at $(T_c + T_a)/2$ (kPa)
VPD_x	= $(e_b^* - e_a)$, vapor pressure deficit of the air at $(T_a + f_0)$ (kPa)
z_{om}	= roughness length for momentum (m)
z_{oh}	= scalar roughness for heat (m)
z	= height above the surface at which U and T_a are measured (m)

tions can be used to provide information at intermediate states with minimal on-site measurements. This simple approach shows promise for estimation of evapotranspiration rates and relative plant stress for partially vegetated fields.

In order to set the stage for the description of this approach, it is necessary to first review the well-known theory and application of the CWSI (Appendix). Readers are encouraged to review the Appendix before proceeding, because the next sections have numerous references to theory, equations, and scientific notation presented in the Appendix. To facilitate cross-referencing between the Appendix and the main text, many of the scientific symbols, notation, and associated units have been summarized in Table 1.

THEORY: VEGETATION INDEX / TEMPERATURE (VIT) TRAPEZOID

Application of the CWSI and associated theory has generally been limited to determination of transpiration rates of mature, full-cover crops [Eqs. (A5)–(A8) in the Appendix]. Using Eqs. (A13)–(A15), it has been shown that the theory may also be used for determination of evaporation rates of bare soil. However, for many farm and rangeland management applications, knowledge of evapotranspiration[1] (the sum of transpiration and evaporation rates) is necessary for a field covered only partially be vegetation; and rather than having measurements of canopy temperature (T_c) as required for computation of CWSI, generally only measurements of surface composite temperature [T_s = a weighted average of both T_c and surface soil temperature (T_o)] acquired with an IRT are available. Under these conditions, theoretical evaluation of CWSI based on Eq. (A7) is difficult due to the lack of knowledge of the amount of vegetation cover, and the complex computation of canopy and aerodynamic resistances (r_c and r_a, respectively) for partially vegetated fields. An alternative approach is proposed here to estimate evapotranspiration rates and relative water deficit of partially vegetated crops based on the theoretical foundation of CWSI and several additional assumptions regarding surface energy flux.

The "VIT trapezoid" approach is based on the hypothesis that a trapezoidal shape would result from a plot of measured surface minus air temperatures ($T_s - T_a$) versus vegetation cover (V_c: unitless, ranging from 0 = no vegetation to 1 = full cover as seen from above) (Fig. 1). The vertices of the trapezoid would correspond to 1) well-watered full-cover vegetation, 2) water-stressed full-cover vegetation, 3) saturated bare soil, and 4) dry bare soil. Using the physical energy balance equations described in the Appendix, it is possible to compute the values of the four vertices of the trapezoid for a specific time, day, and crop. That is, for full-cover, well-watered vegetation,

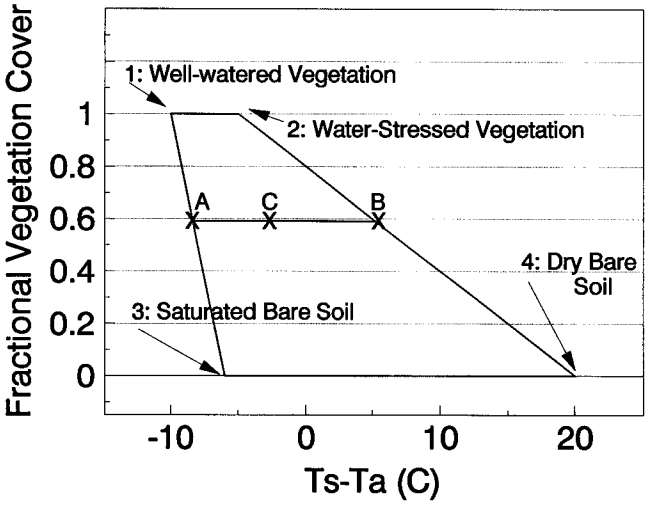

Figure 1. The hypothetical trapezoidal shape that would result from the relation between ($T_s - T_a$) and the fractional vegetation cover (ranging from 0 for bare soil to 1 for full-cover vegetation). With a measurement of ($T_s - T_a$) at point *C*, it would be possible to equate the ratio of actual to potential E_T with the ratio of distances *CB* and *AB*.

$$(T_s - T_a)_1 = [r_a(R_n - G) / C_v][\gamma(1 + r_{cp} / r_a) / \{\Delta + \gamma(1 + r_{cp} / r_a)\}] - [\mathrm{VPD} / \{\Delta + \gamma(1 + r_{cp} / r_a)\}], \quad (1)$$

where the subscript n of $(T_s - T_a)_n$ refers to vertex n in Figure 1 and all other notations are defined in Table 1 and the Appendix. For full-cover vegetation with no available water,

$$(T_s - T_a)_2 = [r_a(R_n - G) / C_v][\gamma(1 + r_{cx} / r_a) / \{\Delta + \gamma(1 + r_{cx} / r_a)\}] - [\mathrm{VPD} / \{\Delta + \gamma(1 + r_{cx} / r_a)\}], \quad (2)$$

where r_{cx} is the canopy resistance associated with nearly complete stomatal closure. For saturated bare soil, where canopy resistance (r_c) = 0 (the case of a free water surface),

$$(T_s - T_a)_3 = [r_a(R_n - G) / C_v][\gamma / (\Delta + \gamma)] - [\mathrm{VPD} / (\Delta + \gamma)], \quad (3)$$

and for dry bare soil, where $r_c = \infty$ (analogous to complete stomatal closure),

$$(T_s - T_a)_4 = [r_a(R_n - G) / C_v]. \quad (4)$$

[1] The term *evapotranspiration* is used here to include the evaporation of water from soil and leaf surfaces and the transpiration of water through leaf stomata. Though in both cases water is "evaporating," and though many prefer to incorporate both evaporation and transpiration into the single term *evaporation*, the distinction is made here for purposes of discussion and presentation of theory.

Theoretically, measurements of $T_s - T_a$ and V_c for a specific field could be plotted within the trapezoid (point C in Fig. 1) and the ratio of distances CB / AB would be equal to the ratio of actual and potential evapotranspiration ($\lambda E_\Gamma / \lambda E_{\Gamma p}$) (derived in the Appendix). Thus, with a simple computation of $\lambda E_{\Gamma p}$, it would be possible to compute actual evapotranspiration rates for a partially vegetated site. The assumptions, input requirements, applications, and sources of error associated with this approach will be addressed in the next sections.

Assumptions

The assumptions associated with the VIT trapezoid warrant some discussion. First, one must assume that $T_s - T_a$ is a linear function of V_c, $(T_c - T_a)$, and $(T_o - T_a)$, where

$$T_s - T_a = V_c(T_c - T_a) + (1 - V_c)(T_o - T_a). \quad (5)$$

This assumption allows straight lines to be drawn between points 2 and 4 and between points 1 and 3 in Figure 1. Kustas et al. (1990) simplified the general equation for the longwave radiative balance of a partially vegetated surface, where

$$(T_s - T_a)^4 = V_c(T_c - T_a)^4 + (1 - V_c)(T_o - T_a)^4. \quad (6)$$

Then, based on measurements of T_c, T_o, T_s, and T_a for a cotton crop in Arizona, they found that T_s could be calculated from T_a, T_c, T_o, and V_c measurements to within ± 1.5°C of the T_s value measured by a sensor mounted on a low-altitude aircraft (flying 150 m above ground level). Similar results were obtained using a model developed by Kimes (1983) that required only information on row orientation and the height and width of the vegetation to produce estimates of the fractional areas of sunlit and shaded soil and sunlit vegetation. These results supported previous findings by Heilman et al. (1981) based on an expression similar to Eq. (6).

A second assumption is that, for a given R_n, VPD, and r_a, variations in $T_c - T_a$ and $T_o - T_a$ are linearly associated with variations in evaporation (E) and transpiration (Γ). That is,

$$T_c - T_a = a + b(\Gamma) \quad (7)$$

and

$$T_o - T_a = a' + b'(E), \quad (8)$$

where a, a', b, and b' are semiempirical coefficients. This assumption has been verified for full cover and bare soil conditions (Vidal and Perrier, 1989) and remains valuable if there are no convective energy exchanges (i.e., no coupling) between soil and vegetation. The relations presented in Eqs. (5)–(8) imply that variations in $T_s - T_a$ are associated with variations in evapotranspiration (E_Γ).[2] Thus, it follows that for a partially vegetated surface,

$$\text{WDI} = 1 - \lambda E_\Gamma / \lambda E_{\Gamma p} = [(T_s - T_a)_m - (T_s - T_a)_r] / [(T_s - T_a)_m - (T_s - T_a)_x], \quad (9)$$

where WDI is the water deficit index (a term coined here for this relation), λE_Γ is the evapotranspiration rate of the surface, $\lambda E_{\Gamma p}$ is the potential evapotranspiration rate, and the subscripts m, x, and r refer to the minimum, maximum, and measured values, respectively [as in Eq. (A9)]. The WDI is operationally equivalent to the CWSI for full-cover canopies, where measurement of $T_s = T_c$. Graphically, WDI is equal to the ratio of distances AC / AB in Figure 1.

There is some evidence that soil and vegetation do not exchange energy separately with the atmosphere, but rather these exchanges are coupled. For example, if the soil is dry and warm relative to cool, transpiring vegetation, the soil will likely lose sensible heat to both the vegetation and the atmosphere. If so, canopy transpiration and soil evaporation cannot be related separately to $(T_c - T_a)$ and $(T_o - T_a)$, respectively, as expressed in Eqs. (7) and (8). In order to account for the exchanges between the soil–vegetation–atmosphere continuum, multicomponent models have been developed in which each "component" is a surface for which exchanges can be expressed as for a single component (Shuttleworth and Wallace, 1985). In general, these models are based on a system of temperatures and resistances between soil, vegetation, and air mass, controlling sensible heat fluxes between the different components. In an approach derived from the one proposed by Shuttleworth and Wallace (1985) and used by Moran et al. (1993), the sensible heat flux was expressed as:

$$H = C_v\{(T_c - T_a)/r_c + (T_o - T_a)/r_o\} / [1 + r_a/r_c + r_a/r_o], \quad (10)$$

where T and r are temperatures and resistances and a, c, and o indices correspond respectively to air, canopy, and soil. Resistances for full-cover vegetation (r_{co}) and bare soil (r_{oo}) per surface unit can be estimated using expressions from Mahrt and Ek (1984) and Shuttleworth and Wallace (1985). The resistances included in Eq. (10) were computed as a function of fractional vegetation cover (V_c), where

$$r_c = r_{co} / V_c \quad \text{and} \quad r_o = r_{oo} / (1 - V_c). \quad (11)$$

Based on this model, an expression analogous to Eq. (9) can be derived,

$$1 - \lambda E_\Gamma / \lambda E_{\Gamma p} = [T_{sm} - T_{sr} + (r_{oo}/r_{co} - 1)V_c(T_{cm} - T_{cr})] / [T_{sm} - T_{sx} + (r_{oo}/r_{co} - 1)V_c(T_{cm} - T_{cx})], \quad (12)$$

where T_c and T_s are canopy and surface temperatures, respectively, and the subscripts m, x, and r refer to minimum, maximum, and measured values, respectively. This equation shows that $1 - \lambda E_\Gamma / \lambda E_{\Gamma p}$ is equal to WDI for bare soil ($V_c = 0$) or full cover ($V_c = 1$). It remains

[2] A distinction between the terms λE_Γ and E_Γ must be clarified; λE_Γ is evapotranspiration rate in energy flux density units (W/m^2) and E_Γ is the same quantity converted to units of rate (mm/h or mm/day).

equal when water deficit conditions of soil and canopy are close together, which is probably the case for many irrigated crops. The sensitivity of the WDI concept to the assumption of noncoupling between the soil and vegetation will be addressed in the next sections.

The VIT trapezoid becomes considerably more useful if the measurements of V_c along the Y-axis are substituted with a spectral vegetation index that is linearly related to V_c. There is evidence that the relation of some spectral vegetation indices with V_c is relatively linear over a large range of V_c values (Huete and Jackson, 1988; Huete, 1988; Moran et al., 1994), though this relation is not unique but rather both crop- and site-specific. Furthermore, Price (1990) demonstrated that vegetation indices computed by band ratios do not satisfy the associative property for area measurements and are thus affected by the spatial resolution of the sensor. Consequently, two sites with the same vegetation cover but different vegetation distribution could yield different values of vegetation index. Though issues such as these must be addressed in each application of the VIT trapezoid, the evidence that the relation is nearly linear over a wide range of values will suffice here for development and demonstration of the concept.

Since it is important for the spectral vegetation index to be sensitive to increases in vegetation cover and insensitive to spectral changes in soil background (such as soil moisture-related differences), the soil-adjusted vegetation index (SAVI) was selected for this demonstration, where

$$\text{SAVI} = (\rho_{\text{NIR}} - \rho_{\text{red}}) / (\rho_{\text{NIR}} + \rho_{\text{red}} + L)(1 + L), \quad (13)$$

and ρ_{NIR} and ρ_{red} are the near-infrared (NIR) and red reflectances, respectively, and L is a unitless constant assumed to be 0.5 for a wide variety of leaf area index (LAI) values (Huete, 1988).

Thus, the VIT trapezoid becomes simply a relation between remotely sensed measurements of surface temperature and a spectral vegetation index derived from the surface reflectance factors in the red and near-infrared spectrum (Fig. 2). Furthermore, for any value of SAVI, it is possible to compute the maximum and minimum $(T_s - T_a)$, by

$$(T_s - T_a)_x = c_0 + c_1(\text{SAVI}) \quad (14)$$

and

$$(T_s - T_a)_m = d_0 + d_1(\text{SAVI}), \quad (15)$$

where c_0 and c_1 are the offset (°C) and slope (°C) of the line connecting points 2 and 4 in Figure 2 and d_0 and d_1 are the offset (°C) and slope (°C) of the line connecting points 1 and 3 in Figure 2. Evaluation of Eqs. (14) and (15) using the VIT trapezoid provides an operational method for computation of WDI [Eq. (9)] for fields ranging from bare soil to fully vegetated.

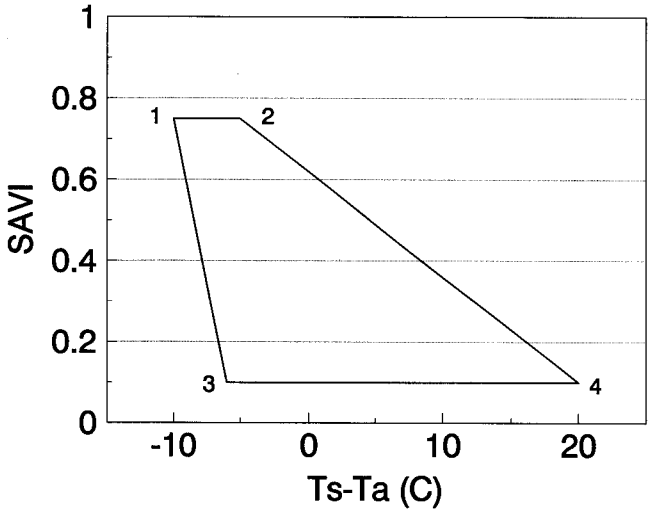

Figure 2. Substitution of the soil-adjusted vegetation index (SAVI) for fractional vegetation cover (Fig. 1) to derive the "VIT trapezoid" based on the relation between $(T_s - T_a)$ and SAVI.

In an operational mode, several more assumptions would make application easier:

Assumption 1: A single value of R_n (measured on-site) can be used in calculations for both bare soil and vegetated targets. Actually, for clear sky conditions, R_n values for a bare soil and for vegetation vary only by the differences in surface albedo and surface temperature, and are dominated by the large value of incoming solar radiation; thus in many cases, the total difference in R_n for bare soil and full-cover vegetation is less than 10% of the actual value of R_n for full-cover vegetation (R. D. Jackson, personal communication). There is other evidence, however, that the differences between R_n for bare soil and vegetated fields can be up to 20% (Daughtry et al., 1990). These differences would apparently be greatest for V_c values between 0.0 and 0.3 and could possibly offset some of the nonlinear response suggested in Eq. (12) for sparsely vegetated fields. Future work should address the computation of bare soil and vegetation R_n values using the techniques proposed by Jackson et al. (1985).

Assumption 2: Values of roughness length (z_o) and displacement height (d_o) for computation of r_a [Eq. A16] can be derived from roughness element height or plant height [h(m)], where $z_o = 0.13h$ and $d_o = 0.67h$ for both bare soil and mature plants. These relations between h, z_o, and d_o were originally derived for rough snow, various grassy surfaces, wheat, fallow, and beets (Paeschke, 1937) and the analysis has been re-

peated by others with the extreme values of z_o/h of 0.06 and 0.24 (Chamberlain, 1966). In fact, the formulation for z_o and d_o involve characteristics other than simply height, such as frontal area, surface density, concentration, and geometrical and drag parameters. Nevertheless, Brutsaert (1982) suggests that such complicated formulations are not necessarily more accurate and are certainly less practical than the z_o/h and d_o/h formulations. Consequently, he recommends that, in the absence of wind profile data, these relations may be used as a first approximation of z_o and d_o.

Assumption 3: Soil heat flux (G) can be estimated as a fraction of R_n dependent only upon V_c (or SAVI). Clothier et al. (1986) found that, for an alfalfa crop in Phoenix Arizona, G/R_n fraction was significantly correlated with the spectral vegetation index and independent of the water content of the soil surface. Similarly, Kustas and Daughtry (1990) reported that G/R_n measured in a cotton crop was linearly correlated with spectral vegetation indices and relatively independent of variations in solar zenith and azimuthal angles throughout the day. Jackson et al. (1987) reported an exponential relation between G/R_n and the vegetation index, though results over a large range on V_c values were nearly linear.

Assumption 4: The kB^{-1} value in Eq. (A17) is a linear function of the product of wind speed and $(T_s - T_a)$ (Kustas et al., 1989) that will likely range from 2 for full-cover crops and wet soil to 8.5 for dry bare soil with moderate wind speeds (Brutsaert, 1982). Brutsaert (1982) showed that the kB^{-1} values for a variety of "permeable-rough," vegetated surfaces ranged from 1 to 3 and could be as high as 12 for a "bluff-rough" surface (his Figure 4.24). Kustas et al. (1989) derived a linear relation between $U(T_s - T_a)$ and kB^{-1} that could be applied to rangeland sites characterized by very sparse vegetation and high surface temperatures. Using extreme approximations for a dry bare soil, where $(T_s - T_a) = 25°C$ and $U = 2$ m s^{-1}, according to Kustas et al. (1989), $kB^{-1} = 0.17(2)(25) = 8.5$.

Input Requirements

In order to compute the vertices of the VIT trapezoid using Eqs. (1)–(4), it is necessary to measure R_n, VPD, and U and T_a at height z for computation of r_a. It is also necessary to estimate the following crop-specific values:

1. Maximum possible plant height and minimum soil roughness [for estimation of z_o and d_o in computation of r_a in Eq. (A16)].
2. Maximum and minimum possible SAVI for full-cover and bare-soil conditions, respectively;
3. Maximum possible LAI [for computation of r_{cx} and r_{cm} from r_{sx} and r_{sm}, respectively, in Eq. (A12)].
4. Maximum and minimum possible stomatal resistances (r_{sx} and r_{sm}).

In many cases, these inputs are known or can be reasonably estimated. Since we are dealing only with the extremes of the VIT trapezoid, it is best to make reasonable but liberal estimates in order to describe the theoretical limits of the trapezoid such that no measurements will ever extend beyond the boundaries [by definition, resulting in values of $(1 - \lambda E_\Gamma / \lambda E_{\Gamma p}) > 1.0$ or < 0.0].

From Trapezoid to Hourglass for Estimation of CWSI

Graphically, one could perceive the VIT trapezoid as being composed of four overlapping triangles (Fig. 3a) and each triangle composed of a family of lines emanating from the main vertex (Figs. 3b–3e). These lines would be defined by variations of Eq. (5) dependent upon limitations on either the value of $(T_o - T_a)$ or $(T_c - T_a)$, where

for triangle A,

$$T_s - T_a = V_c(T_c - T_a) + (1 - V_c)(T_o - T_a)_x, \tag{16}$$

for triangle B,

$$T_s - T_a = V_c(T_c - T_a) + (1 - V_c)(T_o - T_a)_m, \tag{17}$$

for triangle C,

$$T_s - T_a = V_c(T_c - T_a)_m + (1 - V_c)(T_o - T_a), \tag{18}$$

for triangle D,

$$T_s - T_a = V_c(T_c - T_a)_x + (1 - V_c)(T_o - T_a). \tag{19}$$

For example, for a single line in triangle A [Eq. (16)], $(T_c - T_a)$ is a constant value between $(T_c - T_a)_x$ and $(T_c - T_a)_m$, $(T_o - T_a)$ is the maximum possible value defined by Eq. (4), and V_c varies from 0 to 1, resulting in the $(T_s - T_a)$ values that comprise each line within triangle A.

Based on Eqs. (16)–(19) and the location of a single measurement of $(T_s - T_a)$ and SAVI, an hourglass figure can be drawn that defines the range of possible $T_c - T_a$ and $T_o - T_a$ values. For example, consider a measurement that falls within triangles A and D (point x in Fig. 4a). Using Eqs. (16) and (19) with the measurement of $(T_s - T_a)$, the computations of $(T_c - T_a)_x$ and $(T_o - T_a)_x$ [Eqs. (A11) and (A15), respectively], and the value of V_c derived from the SAVI, it is possible to compute the minimum values of $(T_o - T_a)$ and $(T_c - T_a)$ (see points 5 and 6 in Fig. 4b). The range of $T_c - T_a$ illustrated in Figure 4b (range between points 2 and 6) defines the possible CWSI values for the crop [using Eq. (A9)] and, thus, the maximum stress level of the plants. Similar

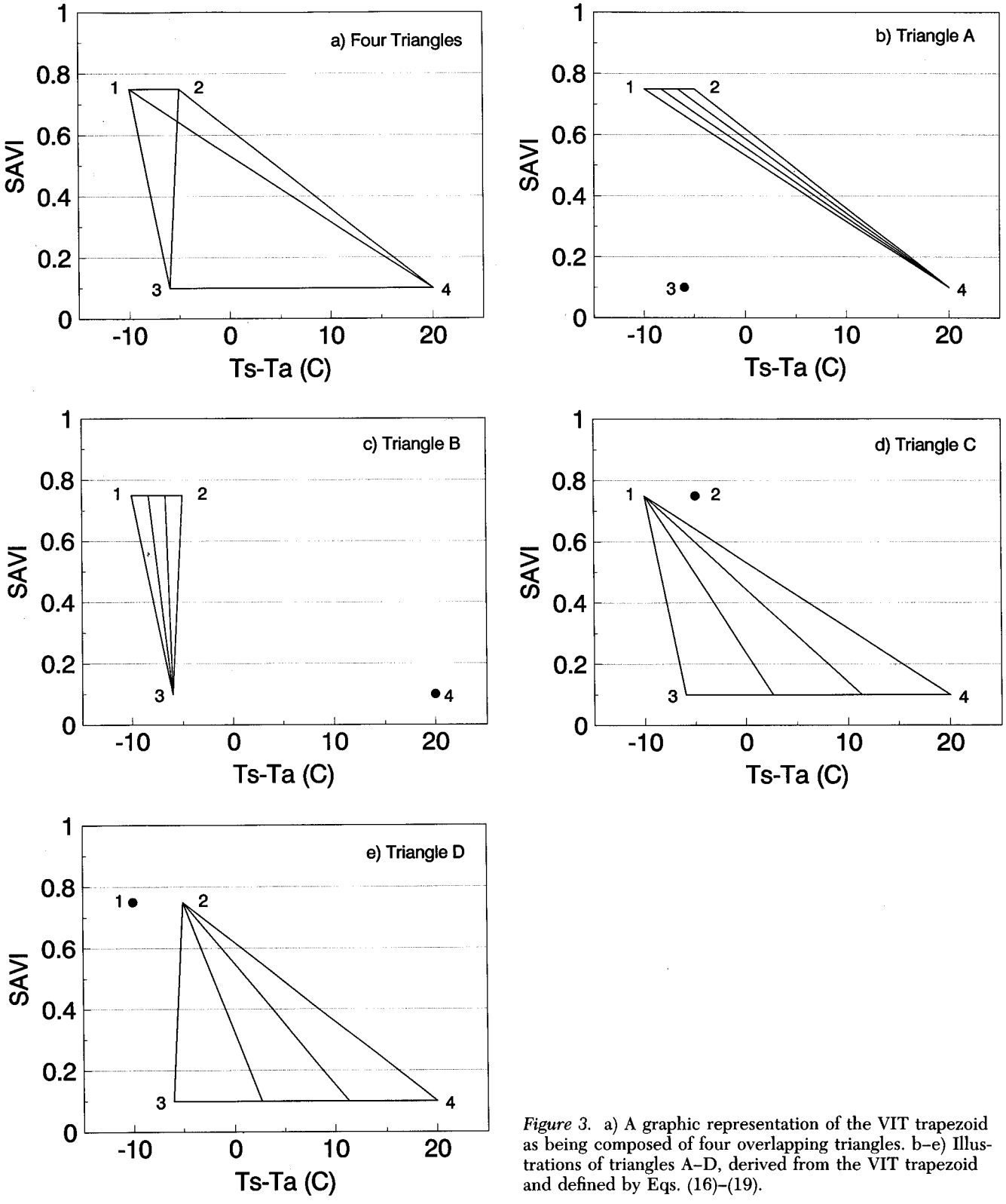

Figure 3. a) A graphic representation of the VIT trapezoid as being composed of four overlapping triangles. b–e) Illustrations of triangles A–D, derived from the VIT trapezoid and defined by Eqs. (16)–(19).

examples could be envisioned for measurement points lying anywhere within the VIT trapezoid. It is apparent the measurements with high SAVI values would result in a low range of $T_c - T_a$ values and measurements with low SAVI values would result in a larger range (illustrated in Fig. 4c).

This knowledge of the *maximum* stress level could be used by farm and rangeland managers to detect

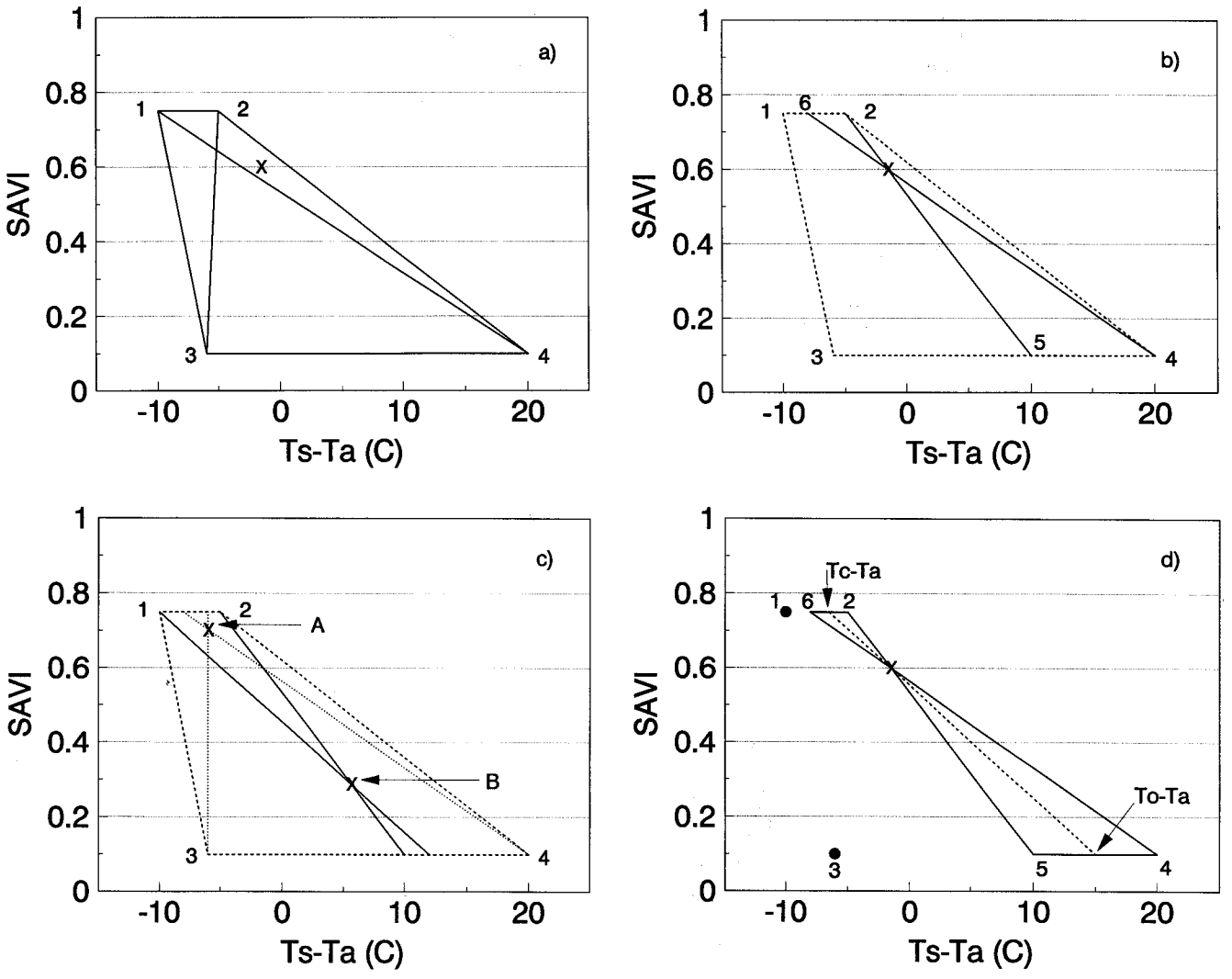

Figure 4. a) Graphic illustration of a measurement of $(T_s - T_a)$ and SAVI in relation to the VIT trapezoid, falling within the limits of triangles A and D. b) The hourglass shape derived from the measurement illustrated in Figure 4a and the lines defined by Eqs. (16) and (19). Dashed lines defined the VIT trapezoid and solid lines define the resultant hourglass. c) Graphic illustration of the hourglass figures associated with two hypothetical points (A and B) within the VIT trapezoid. The dashed lines define the VIT trapezoid, the dotted lines defined the hourglass associated with point A and the solid lines defined the hourglass associated with point *B*. d) Illustration of determination of $(T_c - T_a)$ based on knowledge of $(T_o - T_a)$ and one measurement of $(T_s - T_a)$ within the VIT trapezoid.

relative stress conditions and probable problem areas. Furthermore, with knowledge of a second point within the hour glass (perhaps soil temperature), it would be possible to infer $T_c - T_a$ and pinpoint the CWSI value (illustrated in Fig. 4d).

Sources of Error

The sources of error in the computation of the VIT trapezoid (and the resultant estimates of CWSI using the "hourglass") are similar to those listed by Jackson et al. (1981) for the CWSI. For example, rapidly changing cloud conditions can cause serious error, especially if the air temperature is measured a few minutes before or after the canopy temperature measurements. Furthermore, shaded and sunlit canopies and soils can exhibit different temperatures and the net radiation estimate under such conditions may also be poor.

Errors in meteorological data may also be significant sources of error. Jackson et al. (1981) pointed out that errors in the air temperature measurement enter into the calculation of both $(T_s - T_a)$ and VPD. Inherent errors in estimation of T_s associated with instrument calibration and wrong estimates of emissivity are also a large source of error, particularly when the surface temperature is high.

Finally, errors resulting from the assumption that energy coupling effects between soil and canopy can be ignored [i.e., the difference between Eqs. (9) and (12)]

Table 2. Meteorological and Agronomic Data Related to the Alfalfa Experiment Conducted in 1985 in Phoenix, Arizona (Moran et al., 1989).

Range of R_n	530–600 W m^{-2}
Range of U	1–3.3 m s^{-1}
Range of $(T_s\text{-}T_a)$	−10.6–15.5°C (measured)
Range of r_a	11–74 s m^{-1}
Range of plant height (h)	0.1–1.0 m
Range of SAVI	0.1–0.8 (unitless)
Range of kB^{-1}	2 (full-cover vegetation and wet soil) to 8 (dry bare soil)
Range of G	$0.1R_n$–$0.3R_n$
$\{G/R_n = 0.295\text{–}1.331 \times 10^{-2}(\rho_{NIR}/\rho_{red})$, Clothier et al., 1986$\}$	
Maximum LAI	5 m^2 m^{-2}
r_{sp}	25 s m^{-1}
r_{sx}	1500 s m^{-1}
C_v	1170 J°C^{-1} m^{-3}
z_o	0.13h m
d_o	0.67h m
z	2 m

need to be evaluated. This will be the aim of the concept demonstrations presented in the next sections.

CONCEPT DEMONSTRATION BY SIMULATION

The assumptions of linearity expressed in Eqs. (5)–(8) are an important foundation of the VIT trapezoid concept. These assumptions were tested based on the two-component simulation model described by Eqs. (10)–(12). This analysis was based on measurements made in an alfalfa crop during an experiment conducted in 1985 at the U.S. Water Conservation Laboratory (USWCL) near Phoenix, Arizona (see Table 2 and the experimental description in the next section). The VIT trapezoid was computed using these meteorological data, reasonable values of crop characteristics for well-watered ("maxi-wet") conditions, and values leading to no evapotranspiration when using the model for "maxi-dry" conditions (Fig. 5). Net radiation was assumed to be a constant value, independent of fractional vegetation cover. The ratio of soil heat flux to net radiation (G/R_n) was assumed to vary linearly between 0.3 for bare soil and 0.1 for full-cover vegetation (Clothier et al., 1986).

Simulation Model Results

The first test addressed the linearity of sensible (H) and latent heat flux (λE_T) as a function of fractional vegetation cover (Figs. 6a and 6b). Due to the coupled exchanges and to the nonlinearity of Eq. (10), the simulation results showed that both H and λE_T have nonlinear relations with V_c. This outcome may be explained by the sensible heat transfer between warm soil and cool vegetation that results in an increase in canopy transpiration. This transfer increases when surface heterogeneity increases ($0.7 > V_c > 0.1$) and also when the difference between vegetation and soil temperatures is large.

The next step was to test the linearity of the relation between WDI and λE_T over a range of V_c values from 0 to 1 (Fig. 7). Again, the results suggest that the relation between WDI and $(1 - \lambda E_T / \lambda E_{Tp})$ is not linear over a full range of V_c values. According to this simulation, WDI tends to overestimate the water deficit as defined by $(1 - \lambda E_T / \lambda E_{Tp})$. Furthermore, this overestimation increases with surface heterogeneity, that is, when Eq. (9) differs most from Eq. (12) due to partial-cover vegetation.

In conclusion, results from this two-component model simulation showed a significant nonlinearity between

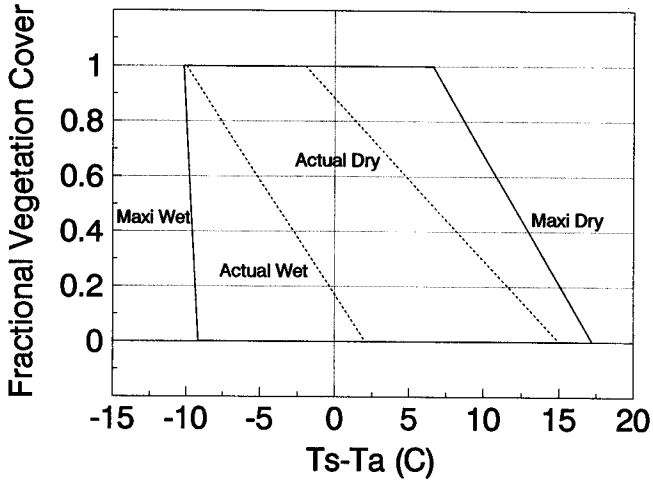

Figure 5. The VIT trapezoid was computed for an alfalfa crop using the meteorological data listed in Table 2 and a derivation of the Shuttleworth / Wallace two-component energy balance simulation. "Maxi-wet" refers to conditions characterized by maximum evapotranspiration and "maxi-dry" refers to conditions in which evapotranspiration = 0. "Actual wet" and "actual dry" conditions were computed based on measurements published by Moran et al. (1992).

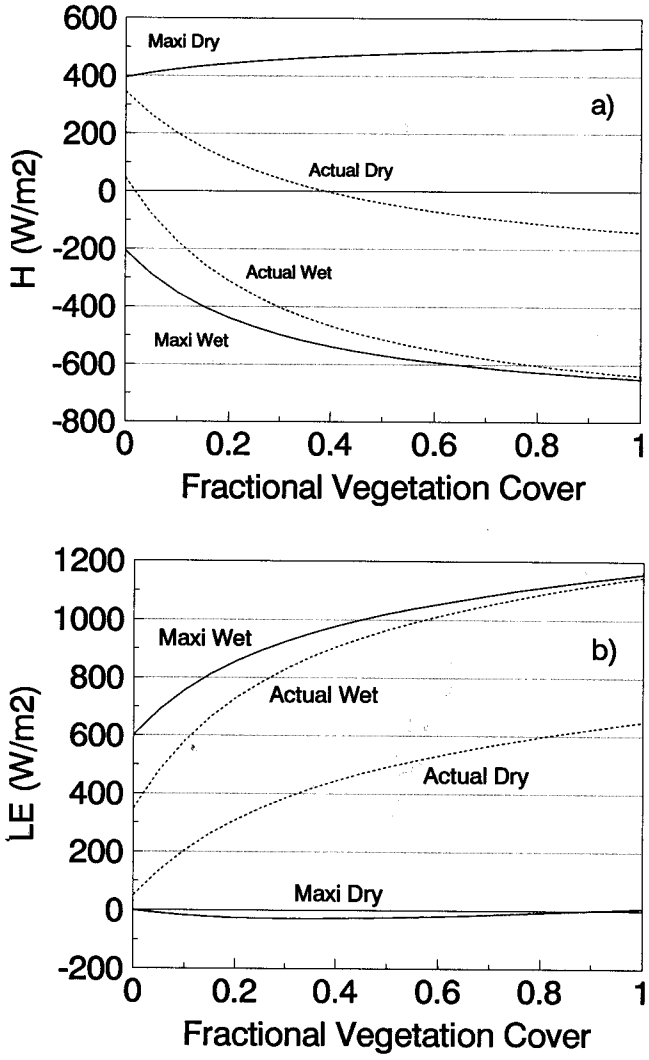

Figure 6. Evaluation of a) H and b) λE_Γ over a range of fractional vegetation cover from 0 to 1 using a deviation of the Shuttleworth / Wallace two-component energy balance simulation model.

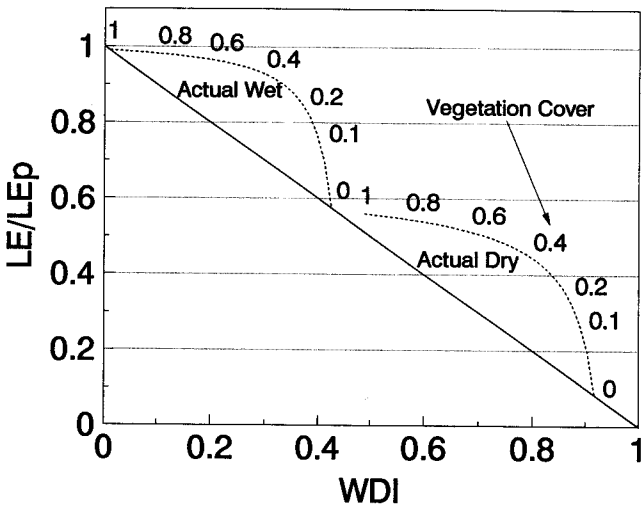

Figure 7. Comparison of WDI and $\lambda E_\Gamma / \lambda E_{\Gamma p}$ over a range of fractional vegetation cover from 0 to 1 using a derivation of the Shuttleworth / Wallace two-component energy balance simulation model.

heat fluxes and vegetation cover, and between WDI and $(1 - \lambda E_\Gamma / \lambda E_{\Gamma p})$, that can essentially be explained by the theoretical soil-to-canopy sensible heat transfer. Consequently, the WDI overestimated the actual water deficit for sparsely vegetated fields. These simulations were helpful in assessing the possible error associated with the noncoupling presumption inherent in the WDI [Eq. (9)]. However, as with all simulation models, there were a variety of assumptions and simplifications required in the derivation and evaluation of Eq. (12). Though simulations are useful for assessing the sensitivity of the WDI derivation, results do not necessarily reflect actual soil–crop–atmosphere interactions. The next section presents a demonstration of the WDI concept based on actual field measurements.

CONCEPT DEMONSTRATION BY EXPERIMENTATION

A demonstration of the VIT trapezoid technique was conducted based on an existing data set from an experiment in an alfalfa (*Medicago sativa* L.) field at the U.S. Water Conservation Laboratory (USWCL) in Phoenix, Arizona. A terse description of the experiment is presented and experimental results follow.

Experiment Description

An experimental alfalfa stand was subdivided into 18 subplots, of which eight were flood irrigated at different intervals to vary levels of water stress and biomass. Four different irrigation regimes were applied to the eight subplots (two replicates each) in each growth cycle: The WET treatment received two irrigations between cuttings; the EARLY treatment was irrigated once, immediately after harvest; the LATE treatment received water midway between cuttings; and the DRY treatment received no supplementary water by irrigation from one harvest until the next. Irrigation treatments were rotated among the 18 subplots to provide a two-harvest cycle rest for plants exposed to water stress during the experiment. The growth interval between harvests ranged from 3.5 weeks in the summer to 9 weeks during winter.

Micrometeorological data were monitored on an hourly basis, and edaphic and agronomic characteristics were observed on a regular basis throughout the experiment. Evaporative water loss was measured with 1 m × 1 m × 1.5 m lysimeters in three treatment plots in the alfalfa field. Methods and previous results from this experiment have been presented by Moran et al. (1989; 1992) and Pinter (1981; 1983).

Surface reflectance factors and temperatures of each treatment plot were measured using a Modular Multispectral Radiometer (MMR) with filters simulating the Landsat Thematic Mapper (TM). Only data from the TM red (0.62–0.69 μm) and NIR (0.78–0.90 μm), and TM thermal (10.42–11.66 μm) will be discussed here. The MMR, deployed using a backpack-type yoke, was used to acquire 12 nadir measurements over a 1 m × 9 m target area in each of the 18 experimental basins (requiring less than 15 min to complete all measurements). The sensor was pointed in a nadir direction, with each lens viewing an area approximately 0.3 m in diameter when the plants were 0.5 m in height. Observations were made several times a week at 10:30 MST to coincide with the time of the Landsat overpass. Reflectances were calculated as the ratio of radiances measured over each alfalfa target to irradiances measured over a 0.6 m × 0.6 m, horizontally positioned, calibrated $BaSO_4$ reference panel (Jackson et al., 1992). Surface temperature data were corrected for surface emissivity, assuming the infrared emissivity of plants is 0.98 and that of this bare soil is 0.94. Since the precise emissivity of the mixed plant / soil surface was unknown, we operationally assumed it was a linear combination of the plant and soil emissivities weighted by percent vegetation cover.

This initial demonstration was limited to one harvest period in 1985 from DOY 154 to DOY 184, when reflectance and temperature measurements were made nearly every day and clear-sky conditions persisted for 28 of 30 days. During this period, the plots containing lysimeters were subjected to EARLY and WET irrigation treatments, respectively.

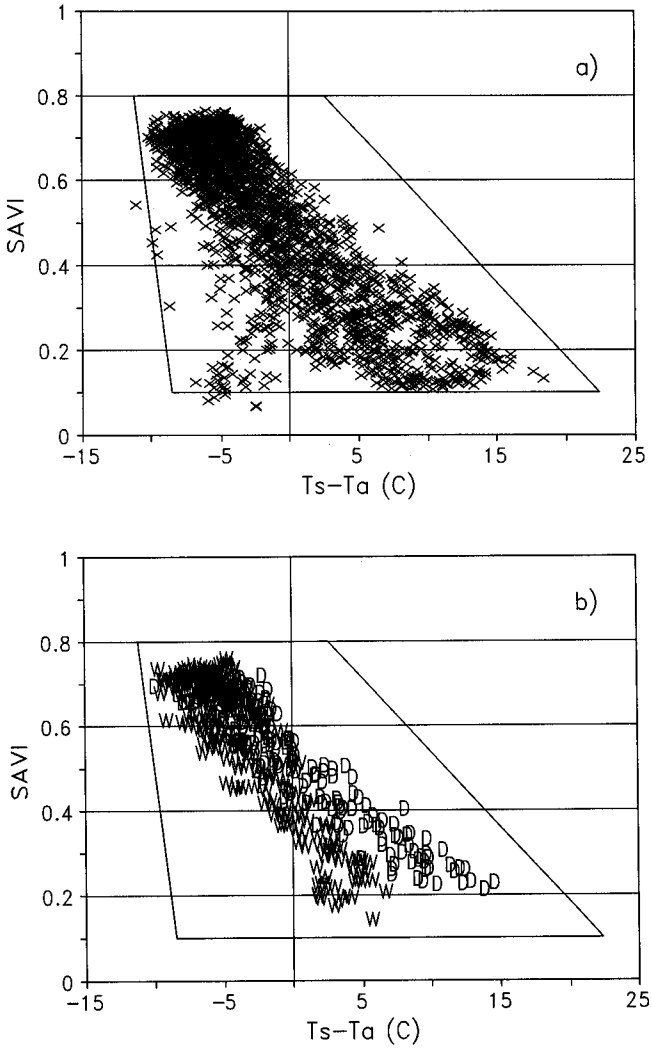

Figure 8. a) Values of $(T_s - T_a)$ and SAVI measured in 18 alfalfa treatment plots over a 10-day period from DOY 161 to DOY 170. The solid lines represent the VIT trapezoid computed based on average values of R_n, VPD, U, and T_a during this period and estimations of maximum and minimum agronomic values for alfalfa (Table 2). b) A subset of data presented in Figure 8a, limited to only the WET (W) and DRY (D) irrigation treatments.

Experimental Results

It is instructive to see the trapezoidal shape realized by the daily measurements of the alfalfa crop. The data presented in Figure 8a include the twelve measurements within each of the 18 treatment basins over a 10-day period during which the crop progressed from a post-harvest stage to full canopy closure [days of year (DOY) 161–170]. The VIT trapezoid was computed based on Eqs. (1)–(4), and average values of R_n, VPD, U and T_a during this period and estimations of maximum and minimum agronomic values for alfalfa (Table 2). During this period, many of the treatment basins were flood-irrigated, resulting in a scatter of points in the lower left region of the trapezoid. A similar scattergram based only on measurements in the WET and DRY treatments (two replicates each) illustrates the physical basis of the trapezoidal shape (Fig. 8b); that is, there were distinct differences in $(T_s - T_a)$ values of WET and DRY treatments early in the growing season (low SAVI values) and discrimination became less distinct as the crop reached maturity (high SAVI values).

Using the VIT trapezoid and Eqs. (9), (14), and (15), WDI was computed for each of two replicates of the WET, LATE, EARLY, and DRY treatment basins (eight basins total) based on the average of the 12 measurements of surface temperature and reflectance factors in each basin. The WDI was affected by two influences during the early and late stages of the growth cycle (Figs. 9a and 9b). For partial canopy (prior to DOY 170), WDI generally decreased with increasing plant cover at rates apparently influenced by available water. For example, WDI for all treatments decreased from DOY 158–168. However, the steepness of the decline was greater for the WET and EARLY treatment plots

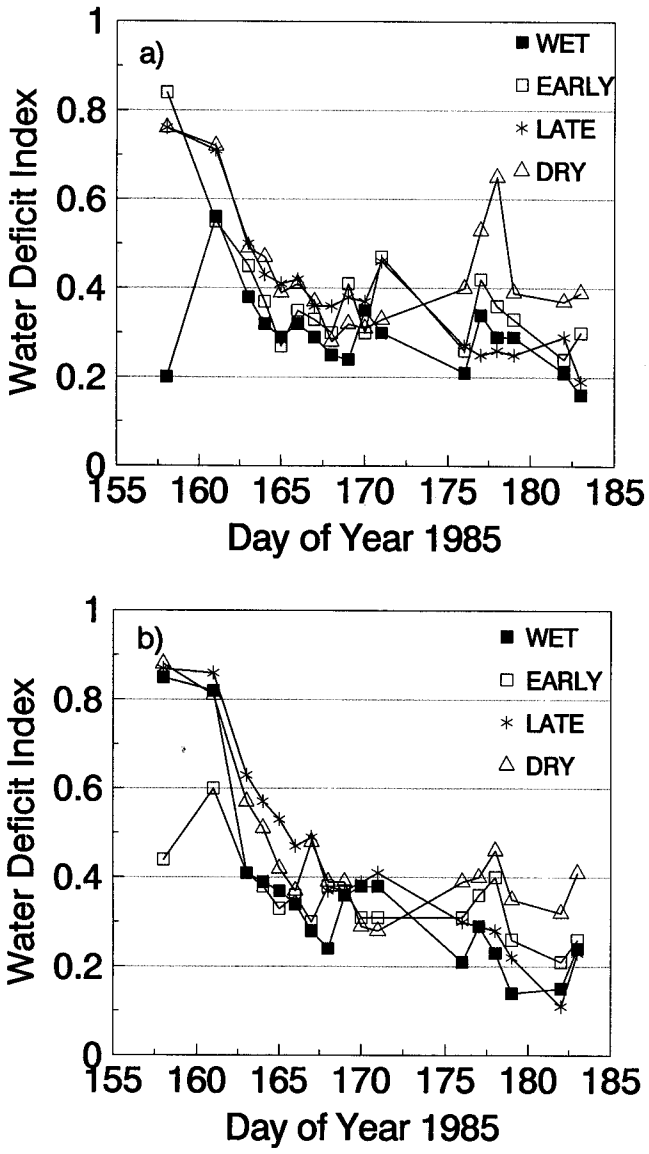

Figure 9. Water deficit index (WDI) values computed for the alfalfa WET, LATE, EARLY, and DRY irrigation treatments over the growth cycle. The two figures (a and b) represent the two replicates of each treatment.

than for the DRY and LATE plots, reflecting the irrigation of the WET and EARLY plots near DOY 158. After 100% vegetation cover was achieved (on or around DOY 170), the steep decline of WDI due to increasing plant cover ceased and the discrimination of the lines appeared to be based solely on irrigation treatment. By the end of the growth cycle, the WDI of the DRY and EARLY treatment plots tended to be higher than that of the WET and LATE plots.

For this alfalfa data set, it was only possible to compare the WDI with CWSI for full-cover conditions, that is, when $T_s = T_c$. This comparison was illustrated for one replicate of each of the four irrigation treatments (Figs. 10a–d). In all cases, the WDI was slightly greater than the theoretical CWSI [Eq. (A7), denoted here as $CWSI_t$]. Both the WDI and theoretical CWSI were substantially greater than the baseline CWSI [Eq. (A18), denoted here as $CWSI_b$], except in the case of very dry conditions associated with the final days of the DRY treatment. Discrepancies between WDI and $CWSI_t$ could be due to errors in the estimation of agronomic parameters for the WDI listed in Table 2.

By definition, it is possible to compare WDI with the ratio E_r / E_{rp}, based on lysimeter measurements of E and computations of E_{rp} (mm h^{-1}). E_{rp} was computed using Eq. (A5) assuming $r_c = r_{cp} = 5$ s m^{-1} and computing r_a for a well-watered, actively growing alfalfa reference crop at full cover (Wright, 1982). For the EARLY and WET treatment basins containing the lysimeters, $(1 - E_r / E_{rp})$ corresponded well with WDI values during the first half of the growth cycle (Figs. 11a and 11b). Toward the end of the growth cycle, $(1 - E_r / E_{rp})$ was slightly greater than WDI for the WET treatment, and substantially greater than WDI for the EARLY treatment. This could be an artifact associated with the limited depth of the lysimeters (1.5 m) relative to the greater depth of roots of mature alfalfa plants. That is, for the WET treatment, the water available to roots of the plants in the lysimeter and in the surrounding field was similar, whereas for the EARLY treatment, it is possible that the plants in the lysimeter were water-stressed toward the end of the growth cycle, and the plants in the surrounding field were still tapping water at a depth below the lysimeter flow. This would account for the good correspondence of the WDI and $(1 - E_r / E_{rp})$ for the WET treatment and for the first half of the EARLY treatment cycle. It would also explain the divergence between WDI and $(1 - E_r / E_{rp})$ in the second half of the EARLY treatment cycle.

In addition to utilizing the VIT Trapezoid for computing WDI and estimates of E_r as shown in Figures 9–11, it is also possible to compute the maximum-possible value of $T_c - T_a$ (and thus maximum CWSI) for a partial cover crop using Eqs. (16)–(19). For two replicates of each of the four irrigation treatments, values of maximum-possible $T_c - T_a$ were computed throughout the growth cycle (Fig. 12). As illustrated in Figure 4c, when the vegetation cover is low, maximum-possible $T_c - T_a$ is equal to $(T_s - T_a)_x$ for full-cover vegetation for all irrigation treatments. As vegetation cover increases, the maximum-possible $T_c - T_a$ values are indicative of the irrigation treatment, with the value for the DRY treatment being much greater than the value for the WET treatment. Translating this value of $T_c - T_a$ to a value of maximum-possible CWSI [using Eqs. (A7) and (A8)], it may be possible to utilize this information for such applications as irrigation scheduling and resource management.

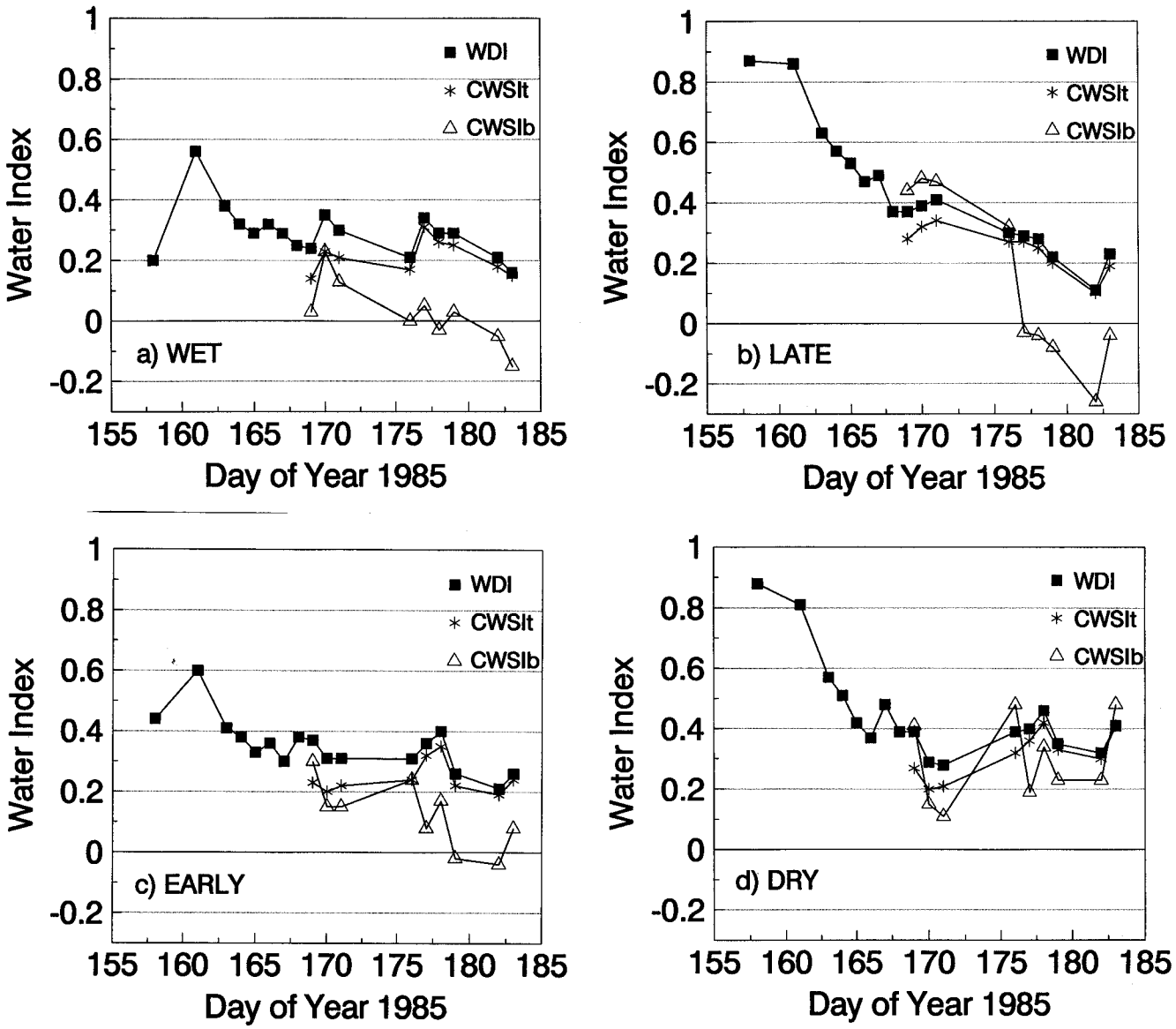

Figure 10. Comparison of the WDI, theoretical CWSI ($CWSI_t$), and baseline CWSI ($CWSI_b$) for one replicate each of the a) WET, b) LATE, c) EARLY, and d) DRY treatments over the growth cycle.

CONCLUDING REMARKS

The VIT trapezoid and WDI appear to have potential for evaluating evapotranspiration rate and relative field water deficit for both full-cover and partially vegetated sites. This represents an advantage over CWSI which was limited in application to full-cover vegetation. Like CWSI, the WDI requires few input parameters in addition to remotely sensed data, and most input values are either known or can be adequately estimated. Furthermore, the technology exists to provide simultaneous measurements of composite surface temperature and spectral reflectance at local and regional scales with ground-, aircraft-, and satellite-based sensors.

The next step in this concept development would be to conduct a thorough sensitivity analysis to determine the required accuracy of input parameters. This would allow us to determine if reasonable estimates of some model inputs would suffice when more accurate measurements were unavailable. Based on the simulation results, there is a need for further refinement of WDI to take into account coupled flux exchanges between the soil–vegetation–atmosphere continuum.

Future research will also be directed towards combining this general concept with measurements of soil temperature (T_o) to determine values of canopy – air temperature ($T_c - T_a$) from surface-air temperature ($T_s - T_a$).

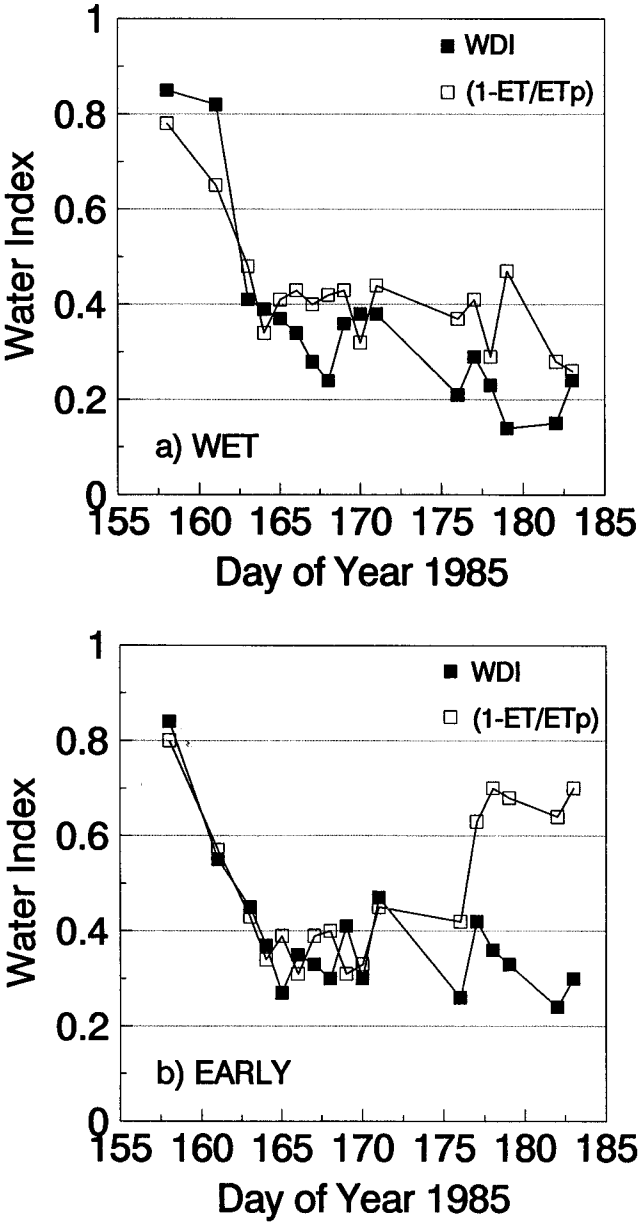

Figure 11. Comparison of the WDI and values of ($1-E_r/E_{rp}$) for the a) WET and b) EARLY alfalfa treatment plots. E_r was measured by lysimeters located in each plot.

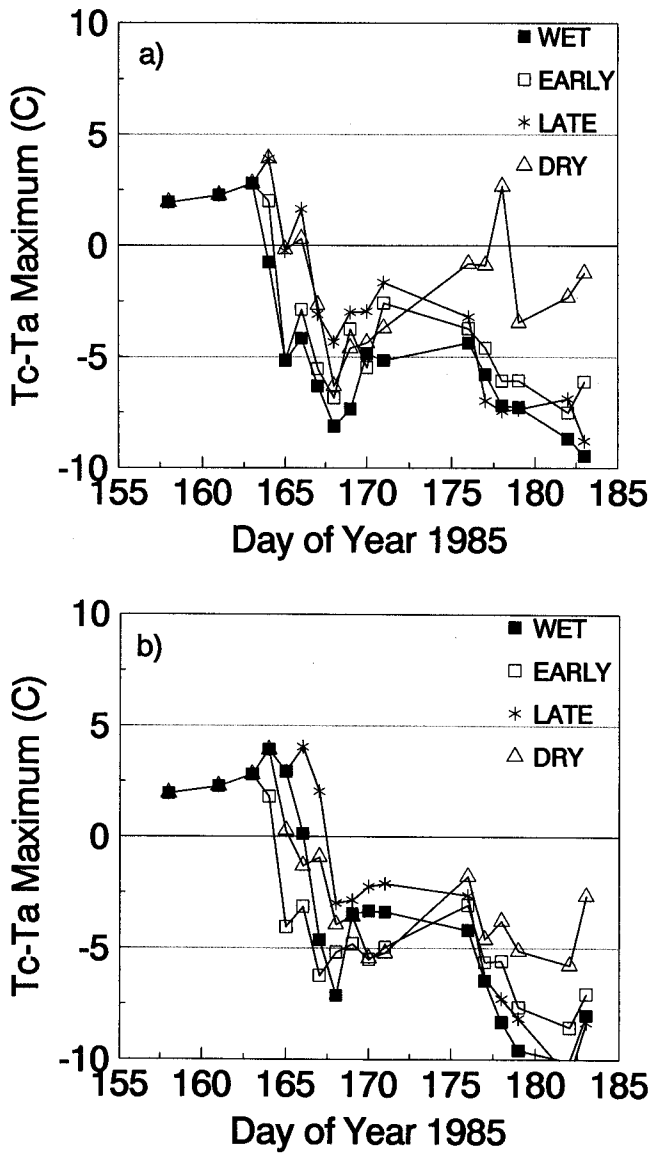

Figure 12. Maximum-possible $T_c - T_a$ values computed for the alfalfa WET, LATE, EARLY, and DRY irrigation treatments over the growth cycle based on the VIT trapezoid and Eqs. (16)–(19). The two figures (a and b) represent the two replicates of each treatment.

Soil temperature could be measured on-site or estimated from ancillary microwave images, when available. This would allow a direct computation of CWSI for both full-cover vegetation and sparsely vegetated fields.

APPENDIX: THEORY AND APPLICATION OF CROP WATER STRESS INDEX (CWSI)

Energy Balance Considerations

The energy balance for a crop was given by Monteith (1973) as

$$R_n = G + H + \lambda E_r, \tag{A1}$$

where R_n is the net radiant heat flux density, G is the soil heat flux density, H is the sensible heat flux density, and λE_r is the latent heat flux density to the air [the product of evapotranspiration rate (E_r) and the heat of vaporization (λ)]. All terms in Eq. (A1) are in units of W m^{-2}, and values of G, H, and λE_r are positive when directed away from the surface. In their simplest forms for dense crops (Penman, 1948; Allen, 1986), H and λE_r can be expressed as:

$$H = C_v(T_c - T_a)/r_a, \tag{A2}$$

$$\lambda E_\Gamma = C_v(\mathrm{VPD}) / [\gamma(r_a + r_c)], \quad \text{(A3)}$$

where C_v is the volumetric heat capacity of air (J °C^{-1} m^{-3}), T_c is the crop foliage temperature (°C), T_a the air temperature (°C), VPD the vapor pressure deficit of the air (kPa), γ the psychrometric constant (kPa °C^{-1}), r_a the aerodynamic resistance (s m^{-1}), and r_c the canopy resistance (s m^{-1}) to vapor transport.

For a full-cover canopy, one could assume that G is negligible and combine Eqs. (A1), (A2), and (A3) to obtain

$$(T_c - T_a) = [r_a R_n / C_v][\gamma(1 + r_c / r_a) / \{\Delta + \gamma(1 + r_c / r_a)\}] - [\mathrm{VPD} / \{\Delta + \gamma(1 + r_c / r_a)\}], \quad \text{(A4)}$$

where Δ is the slope of the saturated vapor pressure–temperature relation (kPa °C^{-1}) (Monteith and Szeicz, 1962).

CWSI—The Theoretical Approach

Jackson et al. (1981) derived the theoretical foundation for the crop water stress index (CWSI) by combining Eqs. (A1)–(A3) to solve for λE_Γ

$$\lambda E_\Gamma = [\Delta R_n + C_v(\mathrm{VPD}) / r_a] / [\Delta + \gamma(1 + r_c / r_a)], \quad \text{(A5)}$$

which is the Penman–Monteith equation for evapotranspiration (Monteith, 1973). Then, taking the ratio of actual (λE_Γ for any r_c) to potential ($\lambda E_{\Gamma p}$ for $r_c = r_{cp}$) latent heat flux density gives

$$\lambda E_\Gamma / \lambda E_{\Gamma p} = [\Delta + \gamma^*] / [\Delta + \gamma(1 + r_c / r_a)], \quad \text{(A6)}$$

where r_{cp} is the canopy resistance at potential evapotranspiration and $\gamma^* = \gamma(1 + r_{cp} / r_a)$. Jackson et al. (1981) defined the CWSI, ranging from 0 (ample water) to 1 (maximum stress), as

$$\mathrm{CWSI} = 1 - \lambda E_\Gamma / \lambda E_{\Gamma p} = [\gamma(1 + r_c / r_a) - \gamma^*] / [\Delta + \gamma(1 + r_c / r_a)]. \quad \text{(A7)}$$

To solve Eq. (A7), a value of r_c / r_a is obtained by rearranging Eq. (A4),

$$r_c / r_a = \{[\gamma r_a R_n / C_v] - [(T_c - T_a)(\Delta + \gamma)] - \mathrm{VPD}\} / \{\gamma[(T_c - T_a) - r_a R_n / C_v]\}, \quad \text{(A8)}$$

and r_c / r_a is substituted into Eq. (A7) to obtain the CWSI.

Another equivalent approach for solution of Eq. (A7) is to compute the theoretical upper and lower limits of $T_c - T_a$ using Eq. (A4) and combine these with the measured $T_c - T_a$ value to compute CWSI as

$$\mathrm{CWSI} = 1 - \lambda E_\Gamma / \lambda E_{\Gamma p} = [(T_c - T_a)_m - (T_c - T_a)_r] / [(T_c - T_a)_m - (T_c - T_a)_x], \quad \text{(A9)}$$

where the subscripts m, x, and r refer to the minimum, maximum, and measured values, respectively. For full-cover, well-watered vegetation,

$$(T_c - T_a)_m = [r_a R_n / C_v][\gamma(1 + r_{cm} / r_a) / \{\Delta + \gamma(1 + r_{cm} / r_a)\}] - [\mathrm{VPD} / \{\Delta + \gamma(1 + r_{cm} / r_a)\}], \quad \text{(A10)}$$

where $r_{cm} = r_{cp}$. For full-cover vegetation with no available water,

$$(T_c - T_a)_x = [r_a R_n / C_v][\gamma(1 + r_{cx} / r_a) / \{\Delta + \gamma(1 + r_{cx} / r_a)\}] - [\mathrm{VPD} / \{\Delta + \gamma(1 + r_{cx} / r_a)\}], \quad \text{(A11)}$$

where r_{cx} is the canopy resistance associated with nearly complete stomatal closure ($r_{cx} \to \infty$). Monteith (1973) suggested the values of r_{cm} and r_{cx} could be obtained from measurements of stomatal resistance (r_s) and leaf area index (LAI), where

$$r_{cm} = r_{sm} / \mathrm{LAI} \quad \text{and} \quad r_{cx} = r_{sx} / \mathrm{LAI}, \quad \text{(A12)}$$

where LAI > 0. Values of minimum and maximum stomatal resistance (r_{sm} and r_{sx}, respectively) are published for many agricultural crops under a variety of atmospheric conditions. If values are not available, reasonable values of r_{sm} = 25–100 s m^{-1} and r_{sx} = 1000–1500 s m^{-1} will not result in appreciable error in Eqs. (A10) and (A11). That is, when r_c is very large or small (relative to r_a), its influence on the magnitude of $(T_c - T_a)$ in Eqs. (A10) and (A11) is small.

Application of CWSI Theory to Bare Soil

The CWSI theory developed by Jackson et al. (1981) can also be applied to bare soil, where Eq. (A9) is used to determine the ratio of actual to potential soil *evaporation* (rather than crop *transpiration*),

$$1 - \lambda E_\Gamma / \lambda E_{\Gamma p} = [(T_o - T_a)_m - (T_o - T_a)_r] / [(T_o - T_a)_m - (T_o - T_a)_x], \quad \text{(A13)}$$

where T_o is soil surface temperature (°C), λE_Γ is evaporation rate of the soil surface (W m^{-2}), and $\lambda E_{\Gamma p}$ is the potential evaporation rate of the soil surface (W m^{-2}). Furthermore, Eq. (A4) can be used to determine soil temperature (T_o) rather than foliage (T_c). For bare soil, the G term is not negligible and, in fact, can approach $0.5R_n$ for dry soils (Idso et al., 1975). Thus, Eq. (A4) can be used to determine $(T_o - T_a)$ by including G in the computation and adjusting the r_c term to values appropriate for bare soil. For saturated bare soil, where $r_c = 0$ (the case of a free water surface),

$$(T_o - T_a)_m = [r_a(R_n - G) / C_v][\gamma / (\Delta + \gamma)] - [\mathrm{VPD} / (\Delta + \gamma)], \quad \text{(A14)}$$

and for dry bare soil, where $r_c = \infty$ (analogous to complete stomatal closure),

$$(T_o - T_a)_x = [r_a(R_n - G) / C_v]. \quad \text{(A15)}$$

Though the index described by Eq. (A13) is similar to the CWSI defined by Eq. (A9), it obviously cannot be termed the *crop water stress index* since it is applied to a surface void of plant life. Rather, the index is indicative of a soil surface water deficit as evidenced by the difference between the actual and potential evaporation from the bare soil, where a value of 1 signifies a large deficit and a value of 0 results when the surface is evaporating at the potential rate ($\lambda E_\Gamma = \lambda E_{\Gamma p}$).

Evaluation of Aerodynamic Resistance

Accurate evaluation of r_a is integral to solution of the CWSI equations, whether applied to crops [Eqs. (A10) and (A11)] or to bare soil [Eqs. (A14) and (A15)]. There are a variety of published equations for calculation of the aerodynamic resistance (r_a), ranging from extremely elementary (a function of wind speed only) to quite rigorous (accounting for atmospheric stability and based on values of wind speed, surface – air temperature[3] ($T_s - T_a$), surface "aerodynamic" roughness, and other parameters). Considering that Eqs. (A10)–(A15) are applicable to surfaces ranging from tall crops to bare soil and from highly stable to highly to unstable conditions, r_a should be computed with a formulation capable of accounting for these differences, such as that presented by Brutsaert (1982),

$$r_a = \{[\ln((z-d_o)/z_{om}) + \ln(z_{om}/z_{oh}) - \Psi_h] \times [\ln((z-d_o)/z_{om}) - \Psi_m]\}/k^2U, \quad \text{(A16)}$$

where U is wind speed (m s^{-1}), z is the height (m) above the surface at which U and T_a are measured (commonly 2 m), d_o is displacement height (m), z_{om} and z_{oh} are the roughness lengths for momentum and heat (m), respectively, and ψ_h and ψ_m are the stability corrections for heat and momentum, respectively (Paulson, 1970). The distinction between the roughness lengths for heat and momentum is necessary due to the dissimilarity between heat and momentum transfer mechanisms. Heat transfer near a surface is controlled primarily by molecular diffusion whereas momentum transfer takes place as a result of both viscous shear and local pressure gradients (Brutsaert, 1982). This difference results in the additional resistance to heat transfer (where $z_{om} > z_{oh}$) associated with the second term in Eq. (A16), which has been expressed as $kB^{-1} = \ln(z_{om}/z_{oh})$ (Chamberlain, 1968). For a uniform vegetative surface, kB^{-1} is observed to be fairly constant, having a value $\simeq 2$ (Garratt and Hicks, 1973).

Kustas et al. (1989) proposed a method to account for the additional heat transfer resistance associated with sparse vegetation. They associated the additional resistance with the differences in transfer processes of heat and momentum by assuming that the kB^{-1} value was not a constant, but rather, a linear function of the product of U and $T_s - T_a$, where

$$kB^{-1} = s_{kB}U(T_s - T_a), \quad \text{(A17)}$$

where s_{kB} is an empirical coefficient, determined to be 0.17 for shrubland vegetation in Owen's Valley, California, and 0.13 for semiarid grassland and shrubland near Tombstone, Arizona (Kustas et al., 1991).

CWSI—The Baseline Approach

Though Jackson et al. (1981) provided a thorough theoretical approach for computation of CWSI, the concept is more universally applied using a semiempirical variation proposed by Idso et al. (1981) based on the "non-water-stressed baseline." This baseline is defined to be the relationship that exists between ($T_c - T_a$) and VPD under conditions of nonlimiting soil moisture, when the plants in question are transpiring at the potential rate. Such non-water-stressed baselines have been determined for many different crops, including aquatic crops and grain crops for both preheading and postheading growth rates (Idso, 1982).

Using the baseline slope [f_1 (°C kPa^{-1})] and intercept [f_0 (°C)] for a specific crop, Eq. (A9) can be written as

$$\text{CWSI} = \{(f_0 + f_1\,\text{VPD}) - (T_c - T_a)_r\}/\{(f_0 - f_1\,\text{VPD}) - (f_0 + f_1\,\text{VPD}_x)\}, \quad \text{(A18)}$$

where $(T_c - T_a)_r$ refers to on-site measurements of canopy and air temperature, $\text{VPD}_x = e_b^* - e_a$, e_b^* is the saturated vapor pressure at $(T_a + f_0)$, and e_a is the vapor pressure of the air. VPD_x differs from VPD by definition, where $\text{VPD} = e^* - e_a$ and e^* is the saturated vapor pressure at $(T_c + T_a)/2$ [see discussion by Jackson et al. (1981)].

The authors would like to acknowledge the many people at the USDA-ARS U.S. Water Conservation Laboratory, Phoenix, Arizona, who participated in the design and implementation of the alfalfa experiment, and the arduous data acquisition and archiving processes, particularly Ray Jackson, Paul Pinter, Bob Reginato, Kirk Clawson, Harold Kelly, Stephanie Johnson, Ron Seay, and Terry Mills. We are also grateful to David Shannon for writing the flexible program that allowed us to automatically compile this data subset from the many hundreds of individual data files. Denis Troufleau (CEMAGREF/ENGREF, Montpellier, France) was instrumental in the concept demonstration based on the two-component simulation model. This work would never have been possible without the inspiration and example of Ray Jackson.

[3] It is important to emphasize the differences between T_c, T_o, and T_s. T_c is the foliage or "crop" temperature. T_o is the temperature of the soil surface. T_s is the surface composite temperature, that is, a weighted average of soil and vegetation temperatures. When the surface is completely covered by vegetation, then $T_s = T_c$; and when the surface is bare soil, then $T_s = T_o$. Throughout this discussion, all temperatures are assumed to be kinetic values; that is, all radiometric temperature measurements have been corrected for surface emissivity.

REFERENCES

Allen, R. G. (1986), A Penman for all seasons, *J. Irrig. Drain. Eng.* 112:348–368.

Brutsaert, W. H. (1982), *Evaporation into the Atmosphere*, D. Reidel, London, 299 pp.

Chamberlain, A. C. (1966), Transport of gases to and from grass and grass-like surfaces, *Proc. Roy. Soc. London* A290: 236–265.

Chamberlain, A. C. (1968), Transport of gases to and from surfaces with bluff and wave-like roughness elements, *Quart. J. Roy. Meteorol. Soc.* 94:318–332.

Clothier, B. E., Clawson, K. L., Pinter, P. J., Jr., Moran, M. S., Reginato, R. J., and Jackson, R. D. (1986), Estimation of soil heat flux from net radiation during the growth of alfalfa, *Agric. For. Meteorol.* 37:319–329.

Daughtry, C. S. T., Kustas, W. P., Moran, M. S., et al. (1990), Spectral estimates of net radiation and soil heat flux, *Remote Sens. Environ.* 32:111–124.

Garratt, J. R., and Hicks, B. B. (1973), Momentum, heat and water vapour transfer to and from natural and artificial surfaces, *Quart. J. Roy. Meteorol. Soc.* 99:680–687.

Heilman, J. L., Heilman, W. E., and Moore, D. G. (1981), Remote sensing of canopy temperature at incomplete cover, *Agron. J.* 73:403–406.

Huete, A. R. (1988), A soil-adjusted vegetation index (SAVI), *Remote Sens. Environ.* 27:47–57.

Huete, A. R., and Jackson, R. D. (1988), Soil and atmosphere influences on the spectra of partial canopies, *Remote Sens. Environ.* 25:89–105.

Idso, S. B. (1982), Non-water-stressed baselines: a key to measuring and interpreting plant water stress, *Agric. Meteorol.* 27:59–70.

Idso, S. B., Aase, J. K., and Jackson, R. D. (1975), Net radiation–soil heat flux relations as influenced by soil water variations, *Boundary Layer Meteorol.* 9:113–122.

Idso, S. B., Jackson, R. D., and Reginato, R. J. (1977b), Remote sensing of crop yields, *Science* 196:19–25.

Idso, S. B., Reginato, R. J., and Jackson, R. D. (1977a), An equation for potential evaporation from soil, water and crop surfaces adaptable to use by remote sensing, *Geophys. Res. Lett.* 4:187–188.

Idso, S. B., Jackson, R. D., and Reginato, R. J. (1978), Extending the "degree day" concept of phenological development to include water stress effects, *Ecology* 59:431–433.

Idso, S. B., Jackson, R. D., Pinter, P. J., Jr., Reginato, R. J., and Hatfield, J. L. (1981), Normalizing the stress-degree-day parameter for environmental variability, *Agric. Meteorol.* 24:45–55.

Idso, S. B., Clawson, K. L., and Anderson, M. G. (1986), Foliage temperature: effects of environmental factors with implications for plant water stress assessment and the CO_2 / climate connection, *Water Resour. Res.* 22:1702–1716.

Jackson, R. D. (1982), Canopy temperature and crop water stress, *Adv. Irrig.* 1:43–85.

Jackson, R. D. (1987), The crop water stress index: A second look, in *Proc. Int. Conf. on Measurement of Soil and Plant Water Status*, Utah State Univ., 6–10 July, Logan, UT.

Jackson, R. D., and Pinter, P. J., Jr. (1981), Detection of water stress in wheat by measurement of reflected solar and emitted thermal IR radiation, in *Spectral Signatures of Objects in Remote Sensing*, Institut National de la Recherche Agronomique, Versailles, France, pp. 399–406.

Jackson, R. D., Reginato, R. J., and Idso, S. B. (1977a), Wheat canopy temperature: a practical tool for evaluating water requirements, *Water Resour. Res.* 13:651–656.

Jackson, R. D., Idso, S. B., Reginato, R. J., and Ehrler, W. L. (1977b), Crop temperature reveals stress, *Crop Soils* 29: 10–13.

Jackson, R. D., Idso, S. B., Reginato, R. J., and Pinter, P. J., Jr. (1980), Remotely sensed crop temperatures and reflectances as inputs to irrigation scheduling, in *Proc. ASCE Irrigation and Drainage Div. Spec. Cong. Res. Session "Today's Challenges"*, Am. Soc. Civ. Eng., Boise, ID, ASCE, New York.

Jackson, R. D., Idso, D. B., Reginato, R. J., and Pinter, P. J., Jr. (1981), Canopy temperature as a crop water stress indicator, *Water Resour. Res.* 17:1133–1138.

Jackson, R. D., Hatfield, J. L., Reginato, R. J., Idso, S. B., and Pinter, P. J., Jr. (1983), Estimation of daily evapotranspiration from one time-of-day measurements, *Agric. Water Manage.* 7:351–362.

Jackson, R. D., Pinter, P. J., Jr., and Reginato, R. J. (1985), Net radiation calculated from remote multispectral and ground station meteorological data, *Agric. For. Meteorol.* 35:153–164.

Jackson, R. D., Moran, M. S., Gay, L. W., and Raymond, L. H. (1987), Evaluating evaporation from field crops using airborne radiometry and ground-based meteorological data, *Irrig. Sci.* 8:81–90.

Jackson, R. D., Clarke, T. R., and Moran, M. S. (1992), Bidirectional calibration results for 11 Spectralon and 16 $BaSO_4$ reference reflectance panels, *Remote Sens. Environ.* 40: 231–239.

Kimes, D. S. (1983), Remote sensing of row crop structure and component temperatures using directional radiometric temperatures and inversion techniques, *Remote Sens. Environ.* 13:33–55.

Kustas, W. P., and Daughtry, C. S. T. (1990), Estimation of the soil heat flux / net radiation ratio from spectral data, *Agric. For. Meteorol.* 49:205–223.

Kustas, W. P., Choudhury, B. J., Moran, M. S., et al. (1989), Determination of sensible heat flux over sparse canopy using thermal infrared data, *Agric. For. Meteorol.* 44:197–216.

Kustas, W. P., Choudhury, B. J., and Inoue, Y., et al. (1990), Ground and aircraft infrared observations over a partially-vegetated area, *Int. J. Remote Sens.* 11:409–427.

Kustas, W. P., Goodrich, D. C., Moran, M. S., et al. (1991), An interdisciplinary field study of the energy and water fluxes in the atmosphere-biosphere system over semiarid rangelands: description and some preliminary results, *Bull. Am. Meteorol. Soc.* 72:1683–1705.

Mahrt, L., and Ek, M. (1984), The influence of atmospheric stability on potential evaporation, *J. Climate Appl. Meteorol.* 23:222–234.

Monteith, J. L. (1973), *Principles of environmental physics*, Arnold, London.

Monteith, J. L., and Szeicz, G. (1962), Radiative temperature in the heat balance of natural surfaces, *Quart. J. Roy. Meteorol. Soc.* 88:496–507.

Moran, M. S., Pinter, P. J., Jr., Clothier, B. E., and Allen, S. G. (1989), Effect of water stress on the canopy architecture and spectral indices of irrigated alfalfa, *Remote Sens. Environ.* 29:251–261.

Moran, M. S., Maas, S. J., and Jackson, R. D. (1992), Combining remote sensing and modeling for regional resource monitoring: Part I: Remote evaluation of surface evaporation and biomass, in *Proc. of 1992 ASPRS/ACSM Convention "Monitoring and Mapping Global Change,"* 3–7 August 1992, Washington, DC.

Moran, M. S., Weltz, M. A., Vidal, A., et al. (1993), Evaluating energy balance of semiarid rangeland from combined optical-microwave remote sensing, in *IEEE Topical Symp. on Combined Optical-Microwave Earth and Atmosphere Sensing,* 22–25 March, Albuquerque, NM IEEE, New York, p. 82–85.

Moran, M. S., Clarke, T. R., Kustas, W. P., Weltz, M. A., and Amer, S. A. (1994), Evaluation of hydrologic parameters in semiarid rangeland using remotely sensed spectral data, *Water Resour. Res.*, 30:1287–1297.

Paeschke, W. (1937), Experimentelle Untersuchungen sum Rauhigkeits- and Stabilitätsproblem in der bodennahem Luftschicht, *Beiträge Phys. Freien Atmos.* 24:163–189.

Paulson, C. A. (1970), The mathematical representation of wind speed and temperature profiles in the unstable atmospheric layer, *J. Appl. Meteorol.* 9:857–861.

Penman, H. L. (1948), Natural evaporation from open water, bare soil and grass, *Proc. Roy. Soc. London* A193:120–146.

Pinter, P. J., Jr. (1981), Remote sensing of microclimatic stress, in *Biometeorology in Integrated Pest Management* (Hatfield and Thomason, Eds.) Academic, New York, pp. 101–145.

Pinter, P. J., Jr. (1983), Monitoring the effect of water stress on the growth of alfalfa via remotely sensed observations of canopy reflectance and temperature, in *Proc. 16th Conf. on Agric. and For. Meteorol.*, 26–29 April, Ft. Collins, CO, Am. Meteorol. Soc., Boston, MA, pp. 91–94.

Pinter, P. J., Jr., Stanghellini, M. E., Reginato, R. J., Idso, S. B., Jenkins, A. D., and Jackson, R. D. (1979), Remote detection of biological stresses in plants using infrared thermometry, *Science* 205:585–587.

Price, J. P. (1990), Using spatial context in satellite data to infer regional scale evapotranspiration, *IEEE Trans. Geosci. Remote Sens.* 28:940–948.

Reginato, R. J., Idso, S. B., and Jackson, R. D. (1978), Estimating forage crop production: a technique adaptable to remote sensing, *Remote Sens. Environ.* 7:77–80.

Shuttleworth, W. J., and Wallace, J. C. (1985), Evaporation from sparse crops—an energy combination theory, *Quart. J. Roy. Meteorol. Soc.* 11:839–855.

Tanner, C. B. (1963), Plant temperature, *Agron. J.* 55:210–211.

Vidal, A., and Perrier, A. (1989), Analysis of a simplified relation for estimating daily evapotranspiration from satellite thermal IR data, *Int. J. Remote Sens.* 10:1327–1337.

Wright, J. L. (1982), New evapotranspiration crop coefficients, *J. Irrig. Drain. Eng. Div. ASCE* 108(IR2):57–74.